BIOCHEMISTRY
including biophysical chemistry & molecular biology

Article

pubs.acs.org/biochemistry

Protein Substrate Discrimination in the Quiescin Sulfhydryl Oxidase (QSOX) Family

Jennifer A. Codding, Benjamin A. Israel, and Colin Thorpe*

Department of Chemistry and Biochemistry, University of Delaware, Newark, Delaware 19716-2522, United States

Supporting Information

ABSTRACT: This work explores the substrate specificity of the quiescin sulfhydryl oxidase (QSOX) family of disulfide-generating flavoenzymes to provide enzymological context for investigation of the physiological roles of these facile catalysts of oxidative protein folding. QSOX enzymes are generally unable to form disulfide bonds within well-structured proteins. Use of a temperature-sensitive mutant of ubiquitin-conjugating enzyme 4 (Ubc4′) as a model substrate shows that QSOX activity correlates with the unfolding of Ubc4′ monitored by circular dichroism. Fusion of Ubc4′ with the more stable glutathione-*S*-transferase domain demonstrates that QSOX can selectively introduce disulfides into the less stable domain of the fusion protein. In terms of intermolecular disulfide bond generation, QSOX is unable to cross-link well-folded globular proteins via their surface thiols. However, the construction of a septuple mutant of RNase A, retaining a single cysteine residue, demonstrates that flexible protein monomers can be directly coupled by the oxidase. Steady- and pre-steady-state kinetic experiments, combined with static fluorescence approaches, indicate that while QSOX is an efficient catalyst for disulfide bond formation between mobile elements of structure, it does not appear to have a significant binding site for unfolded proteins. These aspects of protein substrate discrimination by QSOX family members are rationalized in terms of the stringent steric requirements for disulfide exchange reactions.

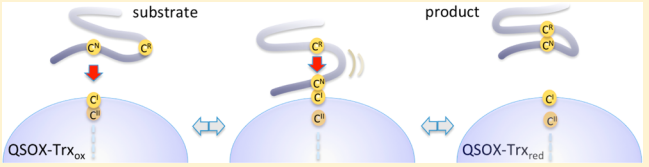

Two types of flavin-linked sulfhydryl oxidases have been identified as participants in the generation of protein disulfide bonds in the secretory apparatus of higher eukaryotes. The endoplasmic reticulum resident sulfhydryl oxidase, endoplasmic reticulum oxidoreductin 1 (Ero1), operates indirectly by oxidizing reduced protein disulfide isomerase (PDI) or a series of related PDI homologues.[1−6] The resulting oxidized PDI proteins serve as the immediate oxidant for nascent chains undergoing oxidative protein folding. Since no known oxidant for protein thiols unerringly generates the correct pairings *de novo*, PDI must intervene a second time in an iterative mode to correct mispairings.[7,8] While this PDI-first model of oxidative folding has gained wide currency, Ron and co-workers recently demonstrated that the Ero1−PDI pathway appears to be nonessential in the mouse.[9] This surprising finding has stimulated a reconsideration of Ero1-independent routes for disulfide bond generation in higher eukaryotes.[9−12]

The quiescin sulfhydryl oxidase (QSOX) family of flavoproteins provides one potential alternative pathway.[12−19] Unlike PDI-first mechanisms for oxidative folding, avian, human, and protist QSOXs interact with unfolded protein substrates directly (Figure 1A), oxidizing ∼2000 thiols/min with K_m values of ∼150 μM per thiol. In contrast to the Ero1 proteins, reduced PDI is not a significant substrate of QSOX.[20] Hence, oxidant and isomerase functions can be segregated; the initial oxidation is promoted by QSOX, leaving reduced PDI to correct mispairings introduced by the oxidase.[20] *In vitro*, this QSOX−PDI system efficiently refolds reduced pancreatic RNase (a four-disulfide protein with 105 disulfide isomers for the fully oxidized protein) and the more complicated riboflavin binding protein (nine native disulfides from more than 34 million disulfide isomers). Neither oxidized PDI nor glutathione redox buffers are necessary for efficient folding in these *in vitro* experiments.[20]

QSOX enzymes represent an ancient fusion between PDI-like thioredoxin (Trx) domains and ERV-like oxidase domains.[13,15,21−23] QSOXs have an N-terminal Trx domain resembling the **a** domain of yeast PDI1p.[12] This domain contains a CxxC motif which serves as the entry point for reducing equivalents[24] (Figure 1B). Metazoan QSOX sequences contain an additional redox-inactive PDI-like Trx domain,[22,24] which is largely, or completely, missing in plants, algae, and protists.[12,22] Following the Trx domain(s), QSOXs contain two helix-rich domains. The domain closest to the C-terminus houses FAD in redox communication with a second CxxC motif (Figure 1B). This Erv-like domain is related to a number of small, stand-alone, dimeric sulfhydryl oxidases including yeast Erv1p and Erv2p, and mammalian ALR.[19,23,25−28] The central helix-rich domain[13] represents a second Erv-like domain which lacks both the bound flavin cofactor and the juxtaposed CxxC motif.[21] Thus, this evolutionary fusion of Trx- and Erv-like domains allows QSOX to efficiently couple the generation of protein disulfide bonds with the reduction of molecular oxygen to hydrogen peroxide.[12,13,18]

Received: March 27, 2012
Revised: May 3, 2012
Published: May 14, 2012

dx.doi.org/10.1021/bi300394w | *Biochemistry* 2012, 51, 4226−4235

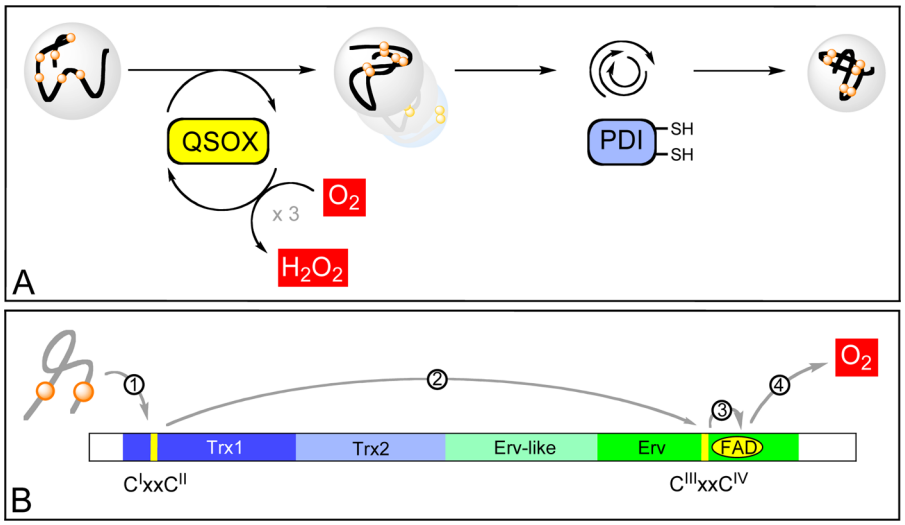

Figure 1. Oxidative protein folding catalyzed by QSOX and PDI and the domain structure of a metazoan QSOX. Panel A shows the segregation of roles between QSOX and reduced PDI. Panel B depicts the domain structure and flow of reducing equivalents in a metazoan QSOX. Reducing equivalents are transferred from the unfolded protein substrate to the $C^{I}xxC^{II}$ motif in the Trx domain,[1] to the $C^{III}xxC^{IV}$ motif in the Erv domain,[2] to flavin,[3] and finally to molecular oxygen.[4]

The precise physiological roles of the QSOX enzymes remain uncertain. Human QSOX1 is abundant in tissues with a heavy secretory load[15,22,29] and is highly up-regulated in prostate[30,31] and pancreatic cancer.[32,33] Immunohistochemistry showed that QSOX1 is found in the ER,[15,34] in the Golgi,[15,34−36] at the cell surface,[37,38] and in the extracellular space.[39−44] Of the two splice variants, QSOX1a retains a C-terminal transmembrane helix and may remain membrane associated, while the shorter QSOX1b form transits the ER and at least some fraction is secreted from cells. Bellen and co-workers suggested that one of the four isoforms of *Drosophila* QSOX generates the majority of the disulfides in the multiple EGF domains of the NOTCH receptor.[45] Chakravarthi et al. showed that a V5-tagged *Hs*QSOX1a long variant accumulated in the Golgi when overexpressed in CHO cells.[35] Furthermore, they suggested that the predominant role of this long form is in late-stage disulfide bond formation, possibly in the maturation of ECM components and in the formation of higher order structures between folded domains.[35] Lake and co-workers also suggested that QSOX can function extracellularly in the activation of matrix metalloproteinases during pancreatic tumor cell invasion.[33]

In light of these interesting recent studies, we explore the reactivity of representative QSOX proteins (avian, human, and trypanosomal) with model substrates to assess whether QSOX can readily introduce intra- and intermolecular disulfide bonds into well-folded protein substrates. Further, we investigate the conditions that promote QSOX-mediated interprotein disulfide bond formation. In addition to providing an enzymological perspective to support ongoing investigation of the biological roles of the QSOX family of oxidases, this work provides new information concerning the likelihood of a binding site in QSOX for unfolded client proteins.

MATERIALS AND METHODS

Materials and Reagents. A synthetic gene for $1C_{65}$-RNase and primers for mutagenesis were ordered from Integrated DNA Technologies. All bacterial culture media components were from Fisher Scientific. PMSF was from Bethesda Research Laboratories; thrombin was from Enzyme Research Laboratories; Pefabloc SC was from Fluka; BLUEstain Protein Ladder was from Goldbio; and IPTG and Broad Range Protein Molecular Markers were from Promega. 4−20% precast linear gradient polyacrylamide gels were from Bio-Rad; Benzamidine Sepharose and PD-10 columns were from GE Healthcare; Amicon Ultra centrifugal filter units were from Millipore; a QuikChange Site-Directed Mutagenesis Kit was from Stratagene; and ProBond Nickel-Chelating Resin was from Invitrogen.

General Methods. Unless otherwise indicated, phosphate buffer containing 50 mM potassium phosphate and 1 mM EDTA adjusted to pH 7.5 was used for all experiments. Proteins were concentrated using Amicon Ultra centrifugal filter units. Visible and ultraviolet spectra were recorded on Hewlett-Packard 8452A or 8453 diode-array spectrophotometers. Steady-state and binding data were plotted and fit using GraphPad Prism software as before.[46] Experiments were performed at least in duplicate. The solvent accessibilities of cysteine residues were calculated using Naccess.[47]

Expression and Purification of QSOX. Avian QSOX was a generous gift from Dr. Karen Hoober and was purified as described earlier.[48] *Trypanosoma brucei* QSOX (*Tb*QSOX) was obtained essentially as described previously,[49] except that the cells were grown to an A_{600} of 3 before induction. *Hs*QSOX1 was obtained as in Heckler et al.[50] with the following modifications which lead to a 5-fold increase in yield. The QSOX1 construct was transferred to a pET28-a plasmid.[50] Following disruption of the Rosetta-gami 2(DE3) cells by French press, the homogenate was briefly sonicated to shear DNA. Washing steps using ProBond nickel chelating resin (Invitrogen) additionally included 10 mM imidazole and were adjusted to pH 7.5. The additional purification steps described earlier,[50] involving a second pass through Ni-NTA resin and a cation exchange column, were omitted. Fractions containing QSOX were concentrated by the addition of ammonium sulfate to 75% saturation. The yellow pellet was redissolved in phosphate buffer and dialyzed against the same buffer. Aliquots (50 μL) of protein supplemented with 20% glycerol were snap frozen in liquid nitrogen and stored at −80 °C.

dx.doi.org/10.1021/bi300394w | *Biochemistry* 2012, 51, 4226−4235

Initially, the avian QSOX was used for further characterization of the substrate specificity of the sulfhydryl oxidases toward cytosolic proteins[18] and for examination of the reactivity of mutants of *E. coli* Trx carrying single surface-accessible cysteine residues (see later). The subsequent availability of the recombinant human QSOX1[50] allowed thermal denaturation and multimerization studies to be performed with this enzyme. The investigation of a protein binding site for QSOX enzymes used both human (2-Trx) and trypanosomal (1-Trx) QSOXs. Rapid reaction kinetic studies required substantial levels of site-directed mutants and were performed with the more readily available 1-Trx *Tb*QSOX.

GST-Ubc4′ Expression. A pGEX-2T-Ubc4′ plasmid (containing the P62S mutation of yeast Ubc4) in TOP10F′ cells was a generous gift from Dr. Kiran Madura, UMDNJ. Protein was expressed in autoinduction medium (ref 51, LBE-5052) containing 50 mg/L ampicillin and 12 mg/L tetracycline. Cells were grown at 25 °C to an A_{600} of 8−10, harvested by centrifugation, and stored at −20 °C.

GST-Ubc4′, Ubc4′, and GST Purification. The purification of Ubc4′ was modified from a previous procedure.[52] Bacterial pellets were resuspended with four volumes of buffer containing 50 mM Tris-HCl, pH 7.5, 50 mM NaCl, 0.25 mM DTT, 1 mM EDTA, 0.72 μg/mL Pefabloc SC, and 0.5 μg/mL leupeptin. The suspension was passed through a French pressure cell twice (at 10 000 psi) followed by 20 s sonication to shear DNA. After centrifugation, the supernatant was added to 2 mL of Glutathione Sepharose beads. The suspension was rocked for 1 h at 4 °C, poured into a column, and washed with three column volumes of 50 mM Tris-HCl, pH 7.5, containing 500 mM NaCl, 0.25 mM DTT, and 1 mM EDTA. The protocols for the purification of GST-Ubc4′, Ubc4′, and GST are described below.

To purify the GST-Ubc4′ construct, the column was developed with 25 mL each of 10 and 20 mM GSH in 20 mM Tris-HCl buffer, pH 7.5, containing 1 mM EDTA and 150 mM NaCl. GST-Ubc4′ fractions were concentrated, washed into phosphate buffer, and stored at −20 °C. To cleave the GST fusion tag from Ubc4′, 2 mL of Glutathione Sepharose beads (as above) was rocked for 6 h with 2 mL of 20 mM Tris-HCl, pH 7.5, containing 150 mM NaCl, 1 mM EDTA, and 30 units of thrombin (Enzyme Research Laboratories). The flow-through was collected, and the column was washed with a second aliquot of the same buffer lacking thrombin. The combined eluates were rocked for 5 min at 4 °C with 60 μL of packed Benzamidine Sepharose (GE Healthcare) in a micro-centrifuge tube. After 1 min centrifugation at 14000*g*, the supernatant was removed and the procedure was repeated with the remaining flow-through, using the same Benzamidine Sepharose beads to minimize loss of Ubc4′ by nonspecific binding. Pefabloc SC (0.08 μg/mL) was added to the combined supernatants to inhibit any residual thrombin. The protein was concentrated and stored in phosphate buffer at −20 °C. GST was recovered from the Glutathione Sepharose column by eluting with 20 mL of 20 mM GSH in phosphate buffer, pH 7.5. GST fractions were concentrated and desalted using a PD-10 column equilibrated with phosphate buffer. Baseline separation between GST and GSH was confirmed by testing small aliquots of eluate with 5,5′-dithiobis(2-nitrobenzoate) (DTNB).[20] GST was stored at −20 °C.

Expression and Purification of Mutant RNases. A synthetic gene, incorporating the N- and C-termini utilized by Raines and colleagues,[53] was designed to encode a septuple cysteine to serine mutant of bovine RNase while retaining C65 (designated $1C_{65}$-RNase). The construct included an N-terminal hexahistidine tag and a nucleotide sequence optimized for expression in *E. coli*. Nucleotide and amino acid sequences for $1C_{65}$-RNase are shown in Figure S1. The gene was subcloned into a pET28-a vector using N-terminal *NcoI* and C-terminal *XhoI* restriction sites and was expressed in BL21*-(DE3) cells. A further C65S mutation of the septuple mutant (designated 0C-RNase) was generated by QuikChange (Stratagene) mutagenesis.

Cells were grown in LB medium supplemented with 15 μg/mL kanamycin at 37 °C until an A_{600} of 0.6 was reached. Protein expression was induced by the addition of 1 mM IPTG, and cells were grown for an additional 3−5 h. Harvested cells were resuspended in 50 mM phosphate buffer, pH 7.5, containing 300 mM NaCl, 10 mM β-ME, 170 μg/mL PMSF, 0.72 μg/mL Pefabloc SC, and 0.5 μg/mL leupeptin. Following French press and sonication steps, the lysate was made 6 M in GnHCl, rocked for 20 min at 4 °C, and centrifuged at 14000*g* for 30 min. The supernatant was added to nickel-chelating resin (10 mL/per 1 mL of packed resin), rocked for 2 h at 4 °C, and poured into a column. The resin was washed with 30 mL of 50 mM phosphate buffer, pH 7.5, containing 300 mM NaCl, 10 mM β-ME, and 6 M GnHCl. The column was developed with 50 mM phosphate buffer, pH 7.5, containing 10 mM β-ME and increasing concentrations of imidazole (30 mL each of 50, 100, and 200 mM imidazole and 20 mL each of 300 and 500 mM imidazole). RNase emerged between 100 and 200 mM imidazole. Fractions were pooled, concentrated, washed into phosphate buffer, and stored at −20 °C (yield: ∼ 6 mg mutant RNase/L).

Preparation of Dansyl- and TNB-Derivatives of $1C_{65}$-RNase. The thawed RNase mutant protein was incubated at 500 μM with equimolar THP in 2 M GnHCl for 10 min (to reduce any disulfide bonds formed during storage) before the addition of 2 mM dansyl-maleimide. After 15 min, the mixture was applied to a PD-10 column equilibrated with phosphate buffer containing 2 M GnHCl, yielding Dansyl-$1C_{65}$-RNase devoid of free thiol groups. The corresponding TNB analogue of $1C_{65}$-RNase was prepared by adding 2 mM DTNB to 150 μM of 1C-RNase pretreated with 300 μM THP. The product was recovered from a PD-10 column as before.

Expression and Purification of Wild Type and Mutant Thioredoxins. *E. coli* Trx was obtained from the pET32a-TRXtag vector (Addgene[54]) and expressed in BL21(DE3)-pLysS cells. Single cysteine mutants were obtained as before and confirmed by sequencing. The following modifications were made to Gross et al.[55] Cells were grown in LB medium containing 50 mg/L ampicillin and 34 mg/L chloramphenicol and induced with 1.0 mM IPTG. Cell pellets were dissolved in 50 mM phosphate buffer, pH 7.5, containing 300 mM NaCl and a protease inhibitor cocktail tablet (Complete, Mini, EDTA free; Roche). The clarified lysate was made 1% in Triton X-100, combined with nickel affinity resin, and rocked for 2 h at 4 °C. The resin was washed with 50 mL of 50 mM phosphate buffer, pH 7.5, containing 300 mM NaCl, 20 mM imidazole, and 10% glycerol, followed by 20 mL of the same buffer lacking NaCl and glycerol. Trx eluted from the column between 30 and 50 mM imidazole and was washed against phosphate buffer prior to storage at −20 °C.

Preparation of Reduced and Oxidized Proteins. *Hs*PDI,[20] wild type and mutant thioredoxins, GST, Ubc4′, and GST-Ubc4′ were reduced before use by incubating each

protein with a 10-fold molar excess of DTT over total thiols for 1 h at 25 °C. $1C_{65}$-RNase was reduced in the presence of 2 M GnHCl. Excess reductant was removed using a PD-10 gel filtration column equilibrated with phosphate buffer. In all cases, quantitative separation of protein and reductant was verified by sampling fractions with DTNB.[20] The four disulfides of wild type RNase A (Sigma) were reduced with DTT by incubation for 1 h at 37 °C in the presence of 6 M GnHCl. rRNase was desalted using a PD-10 column equilibrated with 0.1% acetic acid. Fractions containing rRNase were pooled, lyophilized, and stored at −80 °C. Prior to use, reduced RNase was dissolved in phosphate buffer and standardized for thiol content using DTNB. Fully oxidized PDI was prepared by incubating the protein, as purified, with 2 mM potassium ferricyanide in phosphate buffer for 30 min at 25 °C, followed by gel filtration on a PD-10 column.

Sulfhydryl Oxidase Activity Assays. Oxygen electrode assays were performed as described previously[56] using 5 mM DTT and 50 nM QSOX. The QSOX-driven oxidation of protein thiols was monitored discontinuously by quenching aliquots of the reaction mixture into phosphate buffer containing 1 mM DTNB and 6 M GnHCl. Thiols were quantitated following the absorbance of the TNB anion at 412 nm. Substrate incubations were in phosphate buffer and contained 10 nM bovine catalase to destroy liberated hydrogen peroxide. Initial rates were evaluated after the addition of QSOX.

Thermal Stability. The thermal stability of Ubc4′ was measured using a JASCO J-810 circular dichroism spectrometer. Far-UV (190−260 nm) CD spectra were collected in a 1 mm path length cell containing 6 μM protein and 100 μM TCEP in 10 mM potassium phosphate buffer, pH 7.5, containing 0.2 mM EDTA. A blank was run under identical conditions in the absence of Ubc4′ and was subtracted from the experimental spectra. Three scans were collected at 5 °C increments with 5 min incubation periods at each temperature from 10 to 70 °C (with two additional spectra recorded at 38 and 43 °C). Mean residue ellipticities (degrees cm^2 $dmol^{-1}$) were calculated and plotted at 222 nm as a function of temperature.

QSOX-Mediated Multimerization of Ubc4′. Ubc4′ was added to a concentration of 10 μM in phosphate buffer at 50 °C containing 10 nM catalase and 0−1 μM *Hs*QSOX. Reactions were quenched with 4.3 mM NEM at 50 s, and samples were analyzed by nonreducing SDS-PAGE on a 4−20% gradient gel.

QSOX-Mediated Generation of Intermolecular Disulfides. $1C_{65}$-RNase (200 μM) was incubated in phosphate buffer, 25 °C, containing 10 nM catalase and 500 nM *Hs*QSOX. Aliquots were removed as indicated, quenched into 5 mM *N*-ethylmaleimide (NEM), and analyzed by nonreducing SDS-PAGE.

Fluorescence Measurements. Oxidized PDI or *Tb*QSOX was added from concentrated stocks to Dansyl-$1C_{65}$-RNase (0.5 or 1 μM, respectively, in phosphate buffer, 25 °C). Fluorescence emission was monitored using an Aminco Bowman Series 2 luminescence spectrophotometer (λ_{ex} = 327; λ_{em} = 547). For *Hs*QSOX, 1 μM of the oxidase was titrated with Dansyl-$1C_{65}$-RNase and the fluorescence emission compared to that of a control in the absence of QSOX.

Stopped-Flow Spectrophotometry. The $C^{II}S$ mutant of *Tb*QSOX (10 μM in the syringe) was mixed in phosphate buffer, 25 °C, with 28−114 μM of TNB-$1C_{65}$-RNase using an SF-61 DX2 double-mixing stopped-flow spectrophotometer (Hi-Tech Scientific). Absorbance values at 412 nm were collected in monochromator mode and analyzed using the KinetAsyst 3 software.

RESULTS AND DISCUSSION

Folded Proteins Are Poor Substrates of QSOX. Typical cytosolic proteins from metazoans contain about 1.5% cysteine residues with a range of solvent accessibilities from completely buried to those that lie at the surface. Such proteins do not contain disulfide bonds under normal conditions, and their native folds are not stabilized by these cross-links. While these proteins represent nonphysiological partners of an enzyme that is located within the secretory apparatus or released into the ECM, they present their complement of thiols in a structured environment and provide a tractable experimental model to evaluate the role of substrate flexibility in QSOX activity. In the first part of this work we will examine the reactivity of avian QSOX toward these folded proteins and evaluate their reactivity as the fold is destabilized with chaotrophs. Such experiments cannot be conducted with secreted proteins, whose disulfides are reduced prior to analysis, because the proteins largely or completely unfold following removal of their disulfide bridges. For example, reduction of the four disulfide bonds in RNase A generates a protein which is substantially unstructured in the absence of denaturant.[57−59] Consequently, the eight cysteine residues of rRNase are solvent accessible and react fully with 0.5 mM DTNB in less than 100 ms.[46]

Figure 2 shows that while several of the eight cysteine residues of class I aldolase are solvent accessible,[60,61] they are

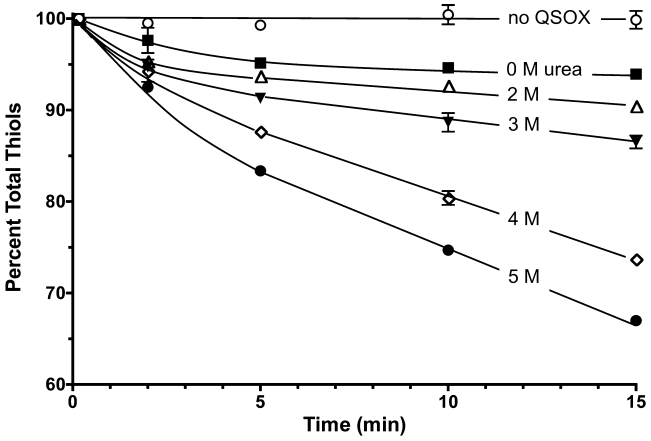

Figure 2. QSOX reactivity toward class I aldolase as a function of urea concentration. The thiol titer of aldolase (80 μM protein thiols in phosphate buffer; set to 100%) was measured discontinuously (see Materials and Methods) at the indicated times in the presence of 100 nM avian QSOX, supplemented with 0, 2, 3, 4, and 5 M urea. The control incubations following aldolase thiols in the absence of QSOX (open circles) showed no significant oxidation up to 15 min. Here, each control time point represents an average over five urea concentrations.

largely unreactive toward avian QSOX. However, thiol oxidation is markedly accelerated when aldolase and QSOX are exposed to increasing concentrations of urea. For perspective, we confirmed that avian QSOX retains from 40 to 60% activity in 5 M urea when assayed using the low molecular weight substrate DTT and the model protein rRNase (Figure S2). A previous report[18] showed that several denatured

dx.doi.org/10.1021/bi300394w | *Biochemistry* 2012, 51, 4226−4235

cytosolic proteins became oxidizable substrates of avian QSOX, and we confirm these earlier findings with adenylosuccinate lyase, alcohol dehydrogenase, lactate dehydrogenase, and pyruvate kinase (Table S1). In sum, structured thiol-containing proteins generally appear to be poor substrates of QSOX.

Thermal Denaturation of Ubc4′ Modulates QSOX Reactivity. As an alternative strategy to disrupting proteins with chaotropes, we explored the reactivity of QSOX toward a model protein substrate that can be reversibly unfolded with increasing temperature.[52] For these experiments, we utilized Ubc4, one of several small ubiquitin-conjugating enzymes from the cytosol of *Saccharomyces cerevisiae*.[62,63] A P62S mutation of the protein (here abbreviated Ubc4′) lowered the melting temperature from 55.9 to 40.5 °C.[52] This latter value lies well within the range of QSOX thermal stability (see later).

Figure 3 shows that folded Ubc4′ is an undetectable substrate of *Hs*QSOX from 10 to 30 °C, although 2 of its 3 cysteine

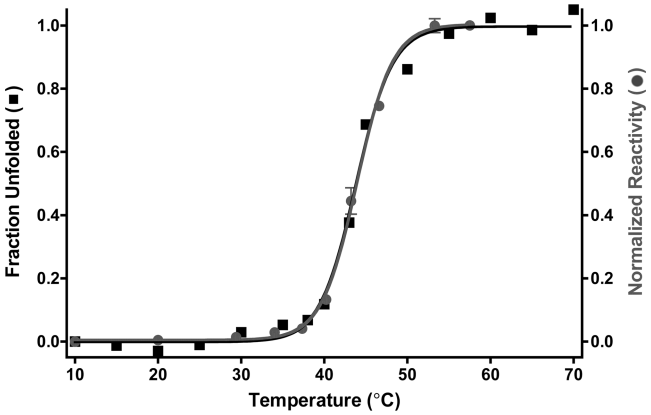

Figure 3. Ubc4′ becomes a substrate of *Hs*QSOX upon thermal unfolding. The thermal denaturation profile for Ubc4′ was monitored by circular dichroism at 222 nm (squares, see Materials and Methods) and the change normalized as shown. Initial rates for Ubc4′ oxidation were established at the indicated temperatures using a discontinuous assay (circles; see Materials and Methods). Control experiments omitting QSOX were performed at each temperature and were subtracted from each reaction. Enzymatic activity was normalized to 1.0 at 60 °C as shown.

residues are appreciably solvent accessible (26 and 55% exposed; Table S2, see Materials and Methods). However, Ubc4′ is significantly oxidized above 35 °C, with a striking transition that closely tracks the cooperative unfolding evaluated by circular dichroism (Figure 3). The midpoint of both curves is 43 °C, in reasonable agreement with the thermal stability reported earlier.[52] However, when Ubc4′ is replaced by rRNase, a protein that is largely a random coil at room temperature,[57−59] a monotonic increase in activity with temperature is encountered (Figure S3). Thus, Ubc4′ only becomes a significant substrate of QSOX when unfolded.

The GST-Ubc4′ fusion protein used in the preparation of Ubc4′ (see Materials and Methods) contains a total of seven cysteine residues, and it was thus of interest to probe the reactivity of the larger protein toward QSOX. For perspective, we first examined the behavior of GST itself. The four cysteine residues of GST are solvent accessible by both experiment[64] and computation (Table S2). This exposure was reported to rationalize the propensity of the protein to form disulfide bridged aggregates which retain comparable enzymatic activity to the monomeric protein.[64] Despite the evident exposure of these surface thiols, *Hs*QSOX shows undetectable reactivity toward GST at 25 °C (data not shown). However, at 50 °C there is a slow decline of thiol titer over the corresponding temperature-matched control in the absence of QSOX (Figure 4) as the thermal transition for unfolding GST is approached.[64]

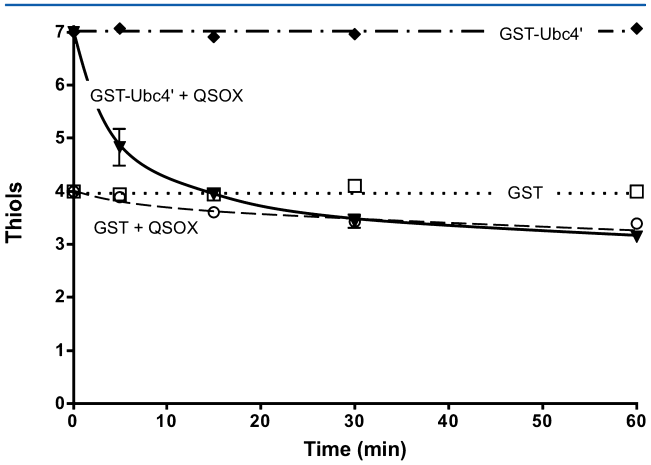

Figure 4. QSOX can preferentially oxidize Ubc4′ thiols in a GST-Ubc4′ fusion protein. The fusion protein (10 μM; 7 total thiols) was incubated in phosphate buffer at 50 °C in the absence and presence of 100 nM *Hs*QSOX (solid diamonds and triangles, respectively). Open circles and squares represent the corresponding incubation of GST (10 μM; 4 thiols) with and without QSOX, respectively.

In the context of the GST-Ubc4′ fusion protein, a rapid oxidation of the three cysteine residues of Ubc4′ is observed at 50 °C, followed by a very slow loss of the remaining four cysteines (compared to the behavior of GST alone; Figure 4). These data demonstrate that QSOX can differentiate between groups of thiols residing in domains of differing conformational stability.

QSOX Generates Interprotein Disulfides in Unstructured Substrates. The quantitative oxidation of an odd number of cysteine residues in the Ubc4′ domain argues for the formation of one or more interprotein disulfide linkages. Accordingly, Ubc4′ was incubated at 50 °C with increasing concentrations of *Hs*QSOX, and the products were sampled by nonreducing PAGE after quenching with excess NEM (see Materials and Methods). Figure 5 shows the progressive appearance of dimers and higher-order multimeric structures of Ubc4′ with increasing QSOX concentrations. At higher oxidase concentrations a significant portion of Ubc4′ did not enter these nonreducing gels, suggesting the formation of large aggregates (data not shown).

Two routes can be envisaged for the covalent association of flexible polypeptide chains containing multiple cysteine residues. In the first, QSOX could drive intramolecular disulfide bond formation, and a subsequent interprotein disulfide exchange would generate the protein cross-links nonenzymatically (depicted in Figure S4). A contribution from this pathway appears highly likely given the general promiscuity of thiol−disulfide exchange reactions between conformationally mobile participants. A second potential route to multimerization would involve a direct intermolecular QSOX-mediated cross-linking between separate chains or assemblies (Figure S4). To unambiguously test the ability of QSOX to catalyze direct intermolecular protein disulfide formation, we sought a substrate that was extensively unfolded at ambient temperatures

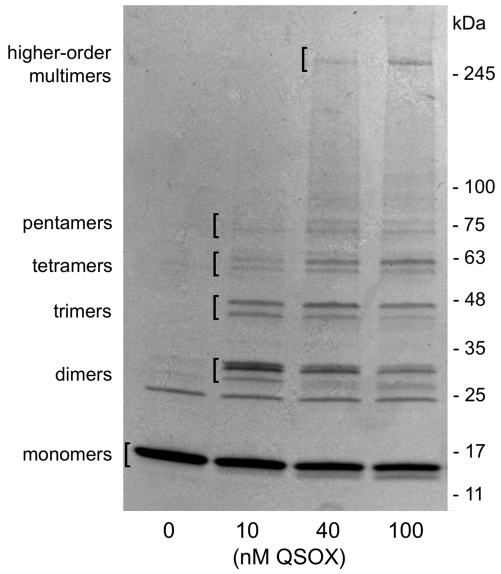

Figure 5. QSOX-mediated multimerization of Ubc4′. Ubc4′ (16.4 kDa) was incubated at 50 °C with the indicated concentrations of *Hs*QSOX. Samples were withdrawn at 50 s, immediately quenched with NEM, and diluted into nonreducing buffer for analysis by SDS-PAGE. Disulfide-linkage isomers are evident in monomer and multimer bands.

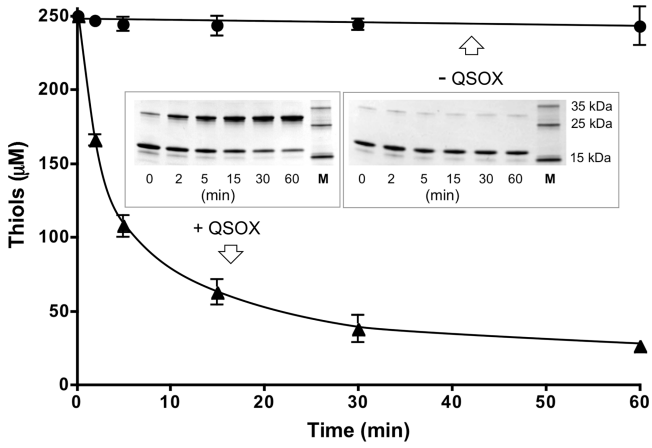

Figure 6. Dimerization of single-cysteine RNase by QSOX. $1C_{65}$-RNase (200 μM) was incubated in phosphate buffer at 25 °C with (triangles) or without (circles) 500 nM *Hs*QSOX. Samples were withdrawn for measurement of thiol titer and for analysis by nonreducing SDS-PAGE after quenching residual free thiols using NEM (see Materials and Methods and inset to the main figure).

and contained a single cysteine residue. The tractability of reduced RNase in a range of experimental approaches led us to the use of a synthetic gene to express a mutant RNase protein, which carried only one of the eight cysteine residues in the wild type protein (see Materials and Methods). In $1C_{65}$-RNase, seven cysteine residues (at positions 26, 40, 58, 72, 84, 95, and 110) were replaced with serine, leaving the remaining cysteine (C65) intact at approximately the middle of the protein. This septuple mutant was conveniently expressed in *E. coli* and purified using an N-terminal His-tag. The construct showed the expected single cysteine by DTNB analysis. Further, $1C_{65}$-RNase proved a substrate of *Hs*QSOX and yielded the corresponding disulfide-bridged dimer (Figure 6). These data clearly demonstrate that QSOX can generate interprotein disulfides directly, at least when the participants are flexible.

QSOX Does Not Readily Generate Interprotein Disulfides between Two Well-Folded Model Proteins. We have already shown that QSOX does not readily oxidize the surface-accessible thiols of GST to yield non-native disulfides at temperatures below the thermal transition for denaturation of this common fusion tag (Figure 4). To complement these data, we wanted a robust, small protein with a single solvent-accessible cysteine residue. We chose *E. coli* Trx[65] because it remains very stable after removal of the catalytically active C32−C35 disulfide bond.[66] Several single cysteine mutants of *E. coli* Trx were prepared (see Materials and Methods and Table S3). The first (C35A) retains the nucleophilic and surface-accessible C32.[65] For the remaining mutants, both native cysteines were removed and single surface-accessible cysteine residues were introduced at positions D10, R73, and N83. Although DTNB reacted readily with these single cysteine variants (not shown), all four proteins (at 200 μM) showed negligible activity with avian QSOX (Table S3). Hence, in the examples examined, QSOX exhibits a very low propensity to couple folded/structured proteins via their surface accessible cysteine side chains. Finally, the inclusion of 3.5 mM reduced glutathione did not significantly increase QSOX-mediated oxidation of these thioredoxin single cysteine mutants (data not shown).

QSOX Lacks a Significant Binding Site for Unfolded Protein Substrates. The experiments presented earlier demonstrate that QSOX is a facile catalyst toward a range of unfolded substrates but exhibits very low activity with well-ordered substrates. One possible explanation is that only unfolded substrates can productively access a binding site on QSOX prior to transferring reducing equivalents to the enzyme (Figure 1B). Three approaches were utilized to evaluate this aspect of QSOX catalysis.

The first set of experiments utilized steady-state kinetics. *Hs*QSOX contains two Trx domains at its N-terminus (Figure 1B), whereas that from *T. brucei* retains only the redox-active Trx domain essential for QSOX's ability to oxidize protein substrates.[12,13,24,49] If either QSOX has a significant binding site for a protein substrate, a non-cysteine-containing version of the same protein should act as a competitive inhibitor of disulfide bond generation. We used native 8-thiol rRNase as the substrate and tested an octuple cysteine to serine variant (0C-RNase, see Materials and Methods) as the potential inhibitor with both human and parasite oxidases. At protein substrate concentrations set to their corresponding K_m values (40 and 45 μM for human and trypanosome QSOX, respectively[49,50]), no significant inhibition of enzyme activity was observed with up to 5-fold higher concentrations of 0C-RNase (Table S4). Since both substrate and putative competitor represent almost identical protein sequences, these data do not support the presence of a significant binding site for rRNase on either of these diverse QSOXs.

A second approach comes from static fluorescence measurements. For these experiments we labeled RNase carrying a single cysteine with a maleimide fluorophore to obtain Dansyl-$1C_{65}$-RNase (see Materials and Methods). PDI was used as a positive control for these experiments because this foldase has been shown to bind a range of peptides and proteins.[8,67] The addition of aliquots of a concentrated solution of PDI to Dansyl-$1C_{65}$-RNase gave the increase in fluorescence shown in Figure 7. These data were fit to a dissociation constant of 3.9 ± 0.4 μM. In contrast, comparable experiments replacing PDI

dx.doi.org/10.1021/bi300394w | *Biochemistry* 2012, 51, 4226−4235

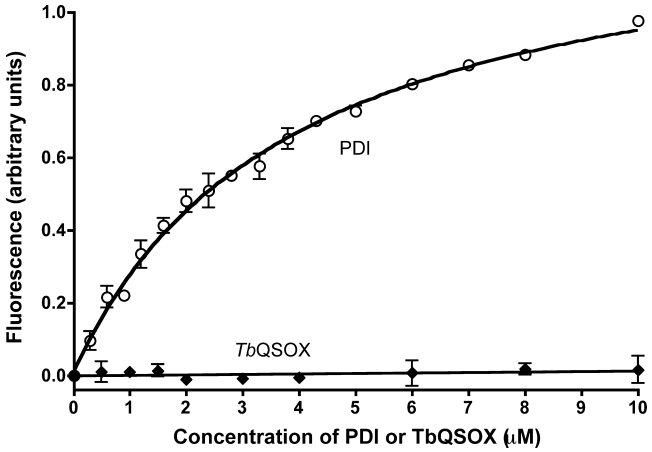

Figure 7. Interaction between Dansyl-1C$_{65}$-RNase and PDI or *Tb*QSOX. Dansyl-1C$_{65}$-RNase (0.5 μM in phosphate buffer) was titrated with the concentrations of oxidized PDI shown (open circles; see the text), and the increase in dansyl fluorescence was fit to a K_d value of 3.9 ± 0.4 μM (see Materials and Methods). A comparable titration with 1 μM Dansyl-RNase was conducted with *Tb*QSOX (closed diamonds) and shows a negligible change of fluorescence.

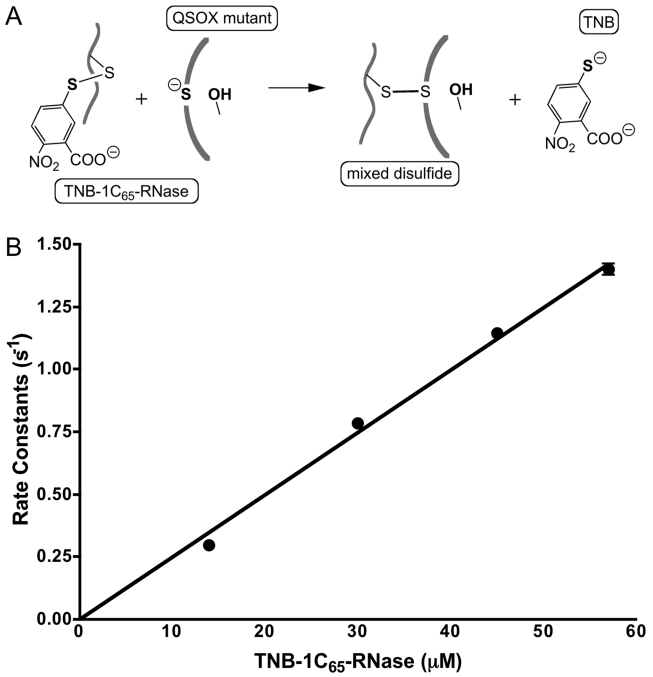

Figure 8. Reactivity of TNB-1C$_{65}$-RNase toward the C^{II}S mutant of *Tb*QSOX. Panel A depicts the reaction between TNB-activated 1C-RNase and the Trx domain of *Tb*QSOX in which C^{II} was mutated to serine. Formation of the mixed disulfide generates the TNB thiolate (absorbing at 412 nm). Panel B plots the pseudo-first-order rate constants of TNB release from 5 μM of the C^{II}S mutant of *Tb*QSOX as a function of the concentration of 1C$_{65}$-RNase.

with *Tb*QSOX showed an insignificant change of fluorescence (Figure 7). The tendency of the human QSOX to aggregate at high protein concentrations[50] precluded using *Hs*QSOX as a titrant; however, experiments in which the order of addition was reversed again provided no evidence for a significant change in fluorescence attributable to complexation (Figure S5).

The final line of evidence comes from rapid reaction experiments. The kinetic mechanism of both a metazoan 2-Trx QSOX[50,68] and the parasite 1-Trx QSOX[49] involves an internal redox reaction between the Trx and Erv domains (e.g., step 2 in Figure 1B). As the concentration of thiol substrates is raised, this internal step eventually becomes rate-limiting, leading to the saturation observed in steady-state kinetics.[49,68] For this reason, the limiting rate observed with increasing concentrations of protein substrates[49] may not reflect the presence of a corresponding binding site on QSOX. To model the first encounter between a protein substrate and QSOX, we adopted the approach shown in Figure 8A. In terms of QSOX, we retained the nucleophilic exchange thiol (C^{I}; Figure 1B) within the Trx domain of *Tb*QSOX but mutated its partner (C^{II}S) to prevent subsequent transfer of reducing equivalents to the Erv domain. As would be expected, this C^{II}S mutant enzyme is essentially inactive with rRNase because the protein substrate cannot directly access the C^{III}–C^{IV} disulfide of the Erv domain.[49] For the surrogate protein substrate we chose 1C$_{65}$-RNase derivatized so that its sole cysteine residue is activated by treatment with DTNB (yielding TNB-1C$_{65}$-RNase). The Trx thiolate can then capture the substrate-TNB derivative with the formation of a mixed disulfide bond (Figure 8A). The generation of a QSOX-RNase mixed disulfide was confirmed by nonreducing SDS-PAGE experiments (not shown). When excess TNB-RNase was used, release of the chromophoric TNB fragment could be fit to a single exponential whose apparent rate constants varied linearly with TNB-1C$_{65}$-RNase concentration (Figure 8B), giving a corresponding bimolecular rate constant of 2.5 × 10^4 M^{-1} s^{-1}. The absence of evidence for saturation under these conditions is again inconsistent with the presence of a strong binding site for unfolded protein substrates.

Steric Requirements for Disulfide Exchange Reactions. The data presented here argue that structural rigidity of protein thiols is a general impediment to their facile oxidation by QSOX enzymes. A rationalization for these observations is based on the relatively stringent steric requirements for disulfide exchange reactions (Figure 9); the attacking thiolate and the two sulfur atoms of the recipient disulfide bond should be collinear.[13,69−71] The redox-active Trx domain of QSOX shows notable sequence similarity to yeast PDI1p.[12,49,50] Like multiple other Trx superfamily members, the C^{I} sulfur is solvent accessible, and the C^{II} sulfur lies buried toward the interior of the domain. In Figure 9, the nucleophilic sulfur atom of the substrate (C^{N}) approaches in line with the C^{I}–C^{II} disulfide of QSOX. The stability of this (C^{N}–C^{I}) mixed disulfide will reflect, in part, the degree to which it can be accommodated sterically against the surface of the QSOX-Trx domain. In step B, a flexible substrate would allow the sulfur atom of the resolving cysteine residue (C^{R}) to approach along the C^{N}–C^{I} axis, leading to product formation (step C). This aspect is likely to provide much of the substrate selectivity exerted by QSOX family members. If the required colinearity cannot be achieved, then product formation will be disfavored. The inability of QSOX to couple surface thiols from two structured proteins (such as those used in the Trx experiments described above) likely reflects the acute steric difficulties associated with resolving the C^{N}–C^{I} mixed disulfide with an incoming thiolate contributed by a second protein. Such steric restraints would be less serious when both protein substrates are flexible, as demonstrated by the QSOX-mediated dimerization of the 1C-RNase described earlier.

dx.doi.org/10.1021/bi300394w | *Biochemistry* 2012, 51, 4226−4235

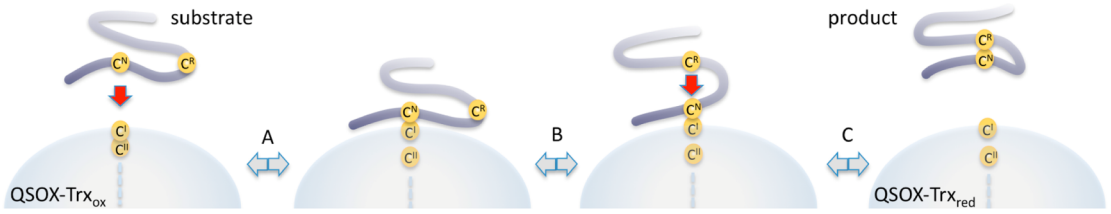

Figure 9. Oxidation of a flexible protein substrate by the redox-active Trx domain of QSOX. The nucleophilic cysteine sulfur atom in a flexible protein substrate is depicted by C^N and that of the corresponding resolving cysteine by C^R. Each disulfide exchange step requires the reacting sulfur atoms to achieve approximate collinearity. Following an initial covalent capture of the substrate in step A, a conformational change in the substrate (step B) is required to bring the resolving sulfur atom in line with the C^N–C^I mixed disulfide.

CONCLUSIONS

Currently, quiescin sulfhydryl oxidases are the most proficient catalysts known for the *de novo* insertion of protein disulfide bonds.[12,13] While the work described here has emphasized the role flexibility plays in accelerating protein disulfide bond formation, this does not preclude the existence of predominantly structured protein substrates of QSOX. In these cases, resolution of the mixed disulfide intermediate would require either preplacement of the resolving cysteine sulfur behind a surface-accessible C^N sulfur or the ability of C^R to attain that geometry following a conformational change between structured elements of the protein. We further demonstrate that QSOX can directly generate interchain disulfide bonds between predominantly unstructured polypeptide chains and discuss steric factors likely to prevent a comparable coupling between thiols on the surface of well-folded proteins. The extent to which these factors impact the behavior of QSOX isoforms as they traverse the secretory pathway and enter the extracellular matrix remains to be established. In sum, this work provides mechanistic context for ongoing studies of the physiological roles of these versatile and widely distributed catalysts of disulfide bond generation in higher eukaryotes.[12,13,19,22,29,38]

ASSOCIATED CONTENT

Supporting Information

Tables S1–S4 providing supplementary tables of kinetic data and cysteine solvent accessibility; Figures S1–S5 representing DNA and protein sequences, kinetic data, and a diagram depicting modes of nonenzymatic and QSOX dimerization. This material is available free of charge via the Internet at http://pubs.acs.org.

AUTHOR INFORMATION

Corresponding Author

*Phone: (302) 831-2689. Fax: (302) 831-6335. E-mail: cthorpe@udel.edu.

Funding

This work was supported in part by National Institutes of Health Grant (GM26643) and USPHS Training Grant 1-T32-GM08550 (J.A.C. and B.A.I.).

Notes

The authors declare no competing financial interest.

ACKNOWLEDGMENTS

We thank Dr. Pumtiwitt McCarthy for preliminary studies, Dr. Ronald Raines for advice concerning RNase expression, Dr. Vamsi Kodali for help with the design of the RNase mutant proteins, and Dr. Kiran Madura and co-workers for a gift of the Ubc4 plasmid and for advice concerning protein purification.

ABBREVIATIONS

β-ME, *β*-mercaptoethanol; Dansyl-, 5-(dimethylamino)-naphthalene-1-sulfonyl-; DTNB, 5,5′-dithiobis(2-nitrobenzoate); ER, endoplasmic reticulum; Ero1, ER oxidoreductin 1; *E. coli*, *Escherichia coli*; GnHCl, guanidine hydrochloride; *Hs*, *Homo sapiens*; IPTG, isopropyl D-thiogalactopyranoside; LB, Luria–Bertani; NEM, *N*-ethylmaleimide; MWCO, molecular weight cutoff; PDI, protein disulfide isomerase; QSOX, quiescin sulfhydryl oxidase; rProtein, reduced protein; RNase A, (rRNase is fully reduced RNase, 0C-RNase is an octuple mutant containing no cysteines, $1C_{65}$-RNase is a septuple mutant retaining C65, and Dansyl-$1C_{65}$-RNase and TNB-$1C_{65}$-RNase are Dansyl- and TNB-derivatives of $1C_{65}$-RNase, respectively); Trx, thioredoxin; TNB, 5-thio-2-nitrobenzoate; THP, tris(hydroxypropyl)phosphine; TCEP, tris(2-carboxyethyl)phosphine; *Tb*, *Trypanosoma brucei*; Ubc4, ubiquitin-conjugating enzyme 4 (Ubc4′ is the P62S mutation).

REFERENCES

(1) Tu, B. P., and Weissman, J. S. (2002) The FAD- and O(2)-dependent reaction cycle of Ero1-mediated oxidative protein folding in the endoplasmic reticulum. *Mol. Cell 10*, 983–994.

(2) Gross, E., Kastner, D. B., Kaiser, C. A., and Fass, D. (2004) Structure of Ero1p, source of disulfide bonds for oxidative protein folding in the cell. *Cell 117*, 601–610.

(3) Vitu, E., Kim, S., Sevier, C. S., Lutzky, O., Heldman, N., Bentzur, M., Unger, T., Yona, M., Kaiser, C. A., and Fass, D. (2010) Oxidative activity of yeast Ero1p on protein disulfide isomerase and related oxidoreductases of the endoplasmic reticulum. *J. Biol. Chem. 285*, 18155–18165.

(4) Frand, A. R., and Kaiser, C. A. (1999) Ero1p oxidizes protein disulfide isomerase in a pathway for disulfide bond formation in the endoplasmic reticulum. *Mol. Cell 4*, 469–477.

(5) Tu, B. P., Ho-Schleyer, S. C., Travers, K. J., and Weissman, J. S. (2000) Biochemical basis of oxidative protein folding in the endoplasmic reticulum. *Science 290*, 1571–1574.

(6) Chambers, J. E., Tavender, T. J., Oka, O. B., Warwood, S., Knight, D., and Bulleid, N. J. (2010) The reduction potential of the active site disulfides of human protein disulfide isomerase limits oxidation of the enzyme by Ero1alpha. *J. Biol. Chem. 285*, 29200–29207.

(7) Wilkinson, B., and Gilbert, H. F. (2004) Protein disulfide isomerase. *Biochim. Biophys. Acta, Proteins Proteomics 1699*, 35–44.

(8) Hatahet, F., and Ruddock, L. W. (2009) Protein Disulfide Isomerase: A Critical Evaluation of Its Function in Disulfide Bond Formation. *Antioxid. Redox Signaling 11*, 2807–2850.

(9) Zito, E., Chin, K. T., Blais, J., Harding, H. P., and Ron, D. (2010) ERO1-beta, a pancreas-specific disulfide oxidase, promotes insulin biogenesis and glucose homeostasis. *J. Cell Biol. 188*, 821–832.

(10) Zito, E., Melo, E. P., Yang, Y., Wahlander, A., Neubert, T. A., and Ron, D. (2010) Oxidative protein folding by an endoplasmic reticulum-localized peroxiredoxin. *Mol. Cell 40*, 787–797.

(11) Tavender, T. J., Springate, J. J., and Bulleid, N. J. (2011) Recycling of peroxiredoxin IV provides a novel pathway for disulphide formation in the endoplasmic reticulum. *EMBO J. 15*, 4185−4197.
(12) Kodali, V. K., and Thorpe, C. (2010) Oxidative protein folding and the Quiescin-sulfhydryl oxidase family of flavoproteins. *Antioxid. Redox Signaling 13*, 1217−1230.
(13) Heckler, E. J., Rancy, P. C., Kodali, V. K., and Thorpe, C. (2008) Generating disulfides with the Quiescin-sulfhydryl oxidases. *Biochim. Biophys. Acta 1783*, 567−577.
(14) Thorpe, C., and Coppock, D. L. (2007) Generating disulfides in multicellular organisms: Emerging roles for a new flavoprotein family. *J. Biol. Chem. 282*, 13929−13933.
(15) Thorpe, C., Hoober, K., Raje, S., Glynn, N., Burnside, J., Turi, G., and Coppock, D. (2002) Sulfhydryl oxidases: emerging catalysts of protein disulfide bond formation in eukaryotes. *Arch. Biochem. Biophys. 405*, 1−12.
(16) Sevier, C. S. (2010) New insights into oxidative folding. *J. Cell Biol. 188*, 757−758.
(17) Hoober, K. L., Glynn, N. M., Burnside, J., Coppock, D. L., and Thorpe, C. (1999) Homology between egg white sulfhydryl oxidase and quiescin Q6 defines a new class of flavin-linked sulfhydryl oxidases. *J. Biol. Chem. 274*, 31759−31762.
(18) Hoober, K. L., Sheasley, S. S., Gilbert, H. F., and Thorpe, C. (1999) Sulfhydryl oxidase from egg white: a facile catalyst for disulfide bond formation in proteins and peptides. *J. Biol. Chem. 274*, 22147−22150.
(19) Sevier, C. S. (2011) Erv2 and Quiescin Sulfhydryl Oxidases: Erv-Domain Enzymes Associated with the Secretory Pathway. *Antioxid. Redox Signaling 16*, 800−808.
(20) Rancy, P. C., and Thorpe, C. (2008) Oxidative Protein Folding in vitro: a Study of the Cooperation between Quiescin-sulfhydryl Oxidase and Protein Disulfide Isomerase. *Biochemistry 47*, 12047−12056.
(21) Alon, A., Heckler, E., Thorpe, C., and Fass, D. (2010) QSOX contains a pseudo-dimer of functional and degenerate sulfhydryl oxidase domains. *FEBS Lett. 584*, 1521−1525.
(22) Coppock, D. L., and Thorpe, C. (2006) Multidomain flavin-dependent sulfhydryl oxidases. *Antioxid. Redox Signaling 8*, 300−311.
(23) Fass, D. (2008) The Erv family of sulfhydryl oxidases. *Biochim. Biophys. Acta 1783*, 557−566.
(24) Raje, S., and Thorpe, C. (2003) Inter-domain redox communication in flavoenzymes of the quiescin/sulfhydryl oxidase family: role of a thioredoxin domain in disulfide bond formation. *Biochemistry 42*, 4560−4568.
(25) Lee, J., Hofhaus, G., and Lisowsky, T. (2000) Erv1p from Saccharomyces cerevisiae is a FAD-linked sulfhydryl oxidase. *FEBS Lett. 477*, 62−66.
(26) Lisowsky, T., Lee, J. E., Polimeno, L., Francavilla, A., and Hofhaus, G. (2001) Mammalian augmenter of liver regeneration protein is a sulfhydryl oxidase. *Dig. Liver Dis. 33*, 173−180.
(27) Gerber, J., Muhlenhoff, U., Hofhaus, G., Lill, R., and Lisowsky, T. (2001) Yeast ERV2p is the first microsomal FAD-linked sulfhydryl oxidase of the Erv1p/Alrp protein family. *J. Biol. Chem. 276*, 23486−23491.
(28) Sevier, C. S., Cuozzo, J. W., Vala, A., Aslund, F., and Kaiser, C. A. (2001) A flavoprotein oxidase defines a new endoplasmic reticulum pathway for biosynthetic disulphide bond formation. *Nat. Cell Biol. 3*, 874−882.
(29) Tury, A., Mairet-Coello, G., Esnard-Feve, A., Benayoun, B., Risold, P. Y., Griffond, B., and Fellmann, D. (2006) Cell-specific localization of the sulphydryl oxidase QSOX in rat peripheral tissues. *Cell Tissue Res. 323*, 91−103.
(30) Ouyang, X., DeWeese, T. L., Nelson, W. G., and Abate-Shen, C. (2005) Loss-of-function of Nkx3.1 promotes increased oxidative damage in prostate carcinogenesis. *Cancer Res. 65*, 6773−6779.
(31) Song, H., Zhang, B., Watson, M. A., Humphrey, P. A., Lim, H., and Milbrandt, J. (2009) Loss of Nkx3.1 leads to the activation of discrete downstream target genes during prostate tumorigenesis. *Oncogene 28*, 3307−3319.
(32) Antwi, K., Hostetter, G., Demeure, M. J., Katchman, B. A., Decker, G. A., Ruiz, Y., Sielaff, T. D., Koep, L. J., and Lake, D. F. (2009) Analysis of the plasma peptidome from pancreas cancer patients connects a peptide in plasma to overexpression of the parent protein in tumors. *J. Proteome Res. 8*, 4722−4731.
(33) Katchman, B. A., Antwi, K., Hostetter, G. H., Demeure, M. J., Watanabe, A., Decker, G. A., Miller, L. J., Von Hoff, D. D., and Lake, D. F. (2011) Quiescin Sulfhydryl Oxidase 1 Promotes Invasion of Pancreatic Tumor cells Mediated by Matrix Metalloproteinases. *Mol. Cancer Res. 9*, 1621−1631.
(34) Tury, A., Mairet-Coello, G., Poncet, F., Jacquemard, C., Risold, P. Y., Fellmann, D., and Griffond, B. (2004) QSOX sulfhydryl oxidase in rat adenohypophysis: localization and regulation by estrogens. *J. Endocrinol. 183*, 353−363.
(35) Chakravarthi, S., Jessop, C. E., Willer, M., Stirling, C. J., and Bulleid, N. J. (2007) Intracellular catalysis of disulphide bond formation by the human sulphydryl oxidase, QSOX1. *Biochem. J. 404*, 403−411.
(36) Mairet-Coello, G., Tury, A., Esnard-Feve, A., Fellmann, D., Risold, P. Y., and Griffond, B. (2004) FAD-linked sulfhydryl oxidase QSOX: topographic, cellular, and subcellular immunolocalization in adult rat central nervous system. *J. Comp. Neurol. 473*, 334−363.
(37) Wittke, I., Wiedemeyer, R., Pillmann, A., Savelyeva, L., Westermann, F., and Schwab, M. (2003) Neuroblastoma-derived sulfhydryl oxidase, a new member of the sulfhydryl oxidase/Quiescin6 family, regulates sensitization to interferon gamma-induced cell death in human neuroblastoma cells. *Cancer Res. 63*, 7742−7752.
(38) Portes, K. F., Ikegami, C. M., Getz, J., Martins, A. P., de Noronha, L., Zischler, L. F., Klassen, G., Camargo, A. A., Zanata, S. M., Bevilacqua, E., and Nakao, L. S. (2007) Tissue distribution of quiescin Q6/sulfhydryl oxidase (QSOX) in developing mouse. *J. Mol. Histol. 39*, 217−225.
(39) Coppock, D. L., Kopman, C., Scandalis, S., and Gillerman, S. (1993) Preferential gene expression in quiescent human lung fibroblasts. *Cell Growth Differ. 4*, 483−493.
(40) Mairet-Coello, G., Tury, A., Fellmann, D., Risold, P. Y., and Griffond, B. (2005) Ontogenesis of the sulfhydryl oxidase QSOX expression in rat brain. *J. Comp. Neurol. 484*, 403−417.
(41) Amiot, C., Musard, J. F., Hadjiyiassemis, M., Jouvenot, M., Fellmann, D., Risold, P. Y., and Adami, P. (2004) Expression of the secreted FAD-dependent sulfydryl oxidase (QSOX) in the guinea pig central nervous system. *Mol. Brain Res. 125*, 13−21.
(42) Ostrowski, M. C., and Kistler, W. S. (1980) Properties of a flavoprotein sulfhydryl oxidase from rat seminal vesicle secretion. *Biochemistry 19*, 2639−2645.
(43) Jaje, J., Wolcott, H. N., Fadugba, O., Cripps, D., Yang, A. J., Mather, I. H., and Thorpe, C. (2007) A flavin-dependent sulfhydryl oxidase in bovine milk. *Biochemistry 46*, 13031−13040.
(44) Zanata, S. M., Luvizon, A. C., Batista, D. F., Ikegami, C. M., Pedrosa, F. O., Souza, E. M., Chaves, D. F., Caron, L. F., Pelizzari, J. V., Laurindo, F. R., and Nakao, L. S. (2005) High levels of active quiescin Q6 sulfhydryl oxidase (QSOX) are selectively present in fetal serum. *Redox Rep. 10*, 319−323.
(45) Tien, A. C., Rajan, A., Schulze, K. L., Ryoo, H. D., Acar, M., Steller, H., and Bellen, H. J. (2008) Ero1L, a thiol oxidase, is required for Notch signaling through cysteine bridge formation of the Lin12-Notch repeats in Drosophila melanogaster. *J. Cell. Biol. 182*, 1113−1125.
(46) Ramadan, D., Rancy, P. C., Nagarkar, R. P., Schneider, J. P., and Thorpe, C. (2009) Arsenic(III) species inhibit oxidative protein folding in vitro. *Biochemistry 48*, 424−432.
(47) Hubbard, S., and Thornton, J. (1993) NACCESS, Computer Program, Department of Biochemistry and Molecular Biology, University College, London.
(48) Hoober, K. L., Joneja, B., White, H. B., III, and Thorpe, C. (1996) A Sulfhydryl Oxidase from Chicken Egg White. *J. Biol. Chem. 271*, 30510−30516.
(49) Kodali, V. K., and Thorpe, C. (2010) Quiescin sulfhydryl oxidase from Trypanosoma brucei: catalytic activity and mechanism of

a QSOX family member with a single thioredoxin domain. *Biochemistry 49*, 2075−2085.
(50) Heckler, E. J., Alon, A., Fass, D., and Thorpe, C. (2008) Human quiescin-sulfhydryl oxidase, QSOX1: probing internal redox steps by mutagenesis. *Biochemistry 47*, 4955−4963.
(51) Studier, F. W. (2005) Protein production by auto-induction in high density shaking cultures. *Protein Expression Purif. 41*, 207−234.
(52) Tongaonkar, P., Beck, K., Shinde, U. P., and Madura, K. (1999) Characterization of a temperature-sensitive mutant of a ubiquitin-conjugating enzyme and its use as a heat-inducible degradation signal. *Anal. Biochem. 272*, 263−269.
(53) delCardayre, S. B., Ribo, M., Yokel, E. M., Quirk, D. J., Rutter, W. J., and Raines, R. T. (1995) Engineering ribonuclease A: production, purification and characterization of wild-type enzyme and mutants at Gln11. *Protein Eng. 8*, 261−273.
(54) Bennett, M. J., Huey-Tubman, K. E., Herr, A. B., West, A. P., Jr., Ross, S. A., and Bjorkman, P. J. (2002) A linear lattice model for polyglutamine in CAG-expansion diseases. *Proc. Natl. Acad. Sci. U. S. A. 99*, 11634−11639.
(55) Gross, E., Sevier, C. S., Heldman, N., Vitu, E., Bentzur, M., Kaiser, C. A., Thorpe, C., and Fass, D. (2006) Generating disulfides enzymatically: reaction products and electron acceptors of the endoplasmic reticulum thiol oxidase Ero1p. *Proc. Natl. Acad. Sci. U. S. A. 103*, 299−304.
(56) Farrell, S. R., and Thorpe, C. (2005) Augmenter of liver regeneration: a flavin dependent sulfhydryl oxidase with cytochrome C reductase activity. *Biochemistry 44*, 1532−1541.
(57) Harrington, W. F., and Sela, M. (1959) A comparison of the physical chemical properties of oxidized and reduced alkylated ribonuclease. *Biochim. Biophys. Acta 31*, 427−434.
(58) Jacob, J., Dothager, R. S., Thiyagarajan, P., and Sosnick, T. R. (2007) Fully reduced ribonuclease A does not expand at high denaturant concentration or temperature. *J. Mol. Biol. 367*, 609−615.
(59) Wang, Y., Trewhella, J., and Goldenberg, D. P. (2008) Small-angle X-ray scattering of reduced ribonuclease A: effects of solution conditions and comparisons with a computational model of unfolded proteins. *J. Mol. Biol. 377*, 1576−1592.
(60) Lai, C. Y., Chen, C., Smith, J. D., and Horecker, B. L. (1971) The number, distribution and functional implication of sulfhydryl groups in rabbit muscle aldolase. *Biochem. Biophys. Res. Commun. 45*, 1497−1505.
(61) Heyduk, T., Michalczyk, R., and Kochman, M. (1991) Long-range effects and conformational flexibility of aldolase. *J. Biol. Chem. 266*, 15650−15655.
(62) Seufert, W., and Jentsch, S. (1990) Ubiquitin-Conjugating Enzymes Ubc4 and Ubc5Mediate Selective Degradation of Short-Lived and Abnormal Proteins. *EMBO J. 9*, 543−550.
(63) Jentsch, S. (1992) The ubiquitin-conjugation system. *Annu. Rev. Genet. 26*, 179−207.
(64) Kaplan, W., Husler, P., Klump, H., Erhardt, J., SluisCremer, N., and Dirr, H. (1997) Conformational stability of pGEX-expressed Schistosoma japonicum glutathione S-transferase: A detoxification enzyme and fusion-protein affinity tag. *Protein Sci. 6*, 399−406.
(65) Holmgren, A. (1995) Thioredoxin structure and mechanism: conformational changes on oxidation of the active-site sulfhydryls to a disulfide. *Structure 3*, 239−243.
(66) Hiraoki, T., Brown, S. B., Stevenson, K. J., and Vogel, H. J. (1988) Structural comparison between oxidized and reduced Escherichia coli thioredoxin. Proton NMR and CD studies. *Biochemistry 27*, 5000−5008.
(67) Klappa, P., Ruddock, L. W., Darby, N. J., and Freedman, R. B. (1998) The b′ domain provides the principal peptide-binding site of protein disulfide isomerase but all domains contribute to binding of misfolded proteins. *EMBO J. 17*, 927−935.
(68) Hoober, K. L., and Thorpe, C. (1999) Egg white sulfhydryl oxidase: Kinetic mechanism of the catalysis of disulfide bond formation. *Biochemistry 38*, 3211−3217.
(69) Rosenfield, R. E., Parthasarathy, R., and Dunitz, J. D. (1977) Directional Preferences of Nonbonded Atomic Contacts with Divalent Sulfur 0.1. Electrophiles and Nucleophiles. *J. Am. Chem. Soc. 99*, 4860−4862.
(70) Fernandes, P. A., and Ramos, M. J. (2004) Theoretical insights into the mechanism for thiol/disulfide exchange. *Chemistry 10*, 257−266.
(71) Bach, R. D., Dmitrenko, O., and Thorpe, C. (2008) Mechanism of thiolate-disulfide interchange reactions in biochemistry. *J. Org. Chem. 73*, 12−21.